Cell

Hexosamine Pathway Metabolites Enhance Protein Quality Control and Prolong Life

Martin S. Denzel,[1,7] Nadia J. Storm,[1,7] Aljona Gutschmidt,[3,4] Ruth Baddi,[1] Yvonne Hinze,[1] Ernst Jarosch,[5] Thomas Sommer,[5,6] Thorsten Hoppe,[3,4] and Adam Antebi[1,2,3,*]

[1]Max Planck Institute for Biology of Ageing, Joseph-Stelzmann-Strasse 9b, Cologne 50931, Germany
[2]Department of Molecular and Cellular Biology, Huffington Center on Aging, Baylor College of Medicine, One Baylor Plaza, Houston, TX 77030, USA
[3]Cologne Excellence Cluster on Cellular Stress Responses in Aging-Associated Diseases (CECAD), University of Cologne, Cologne 50674, Germany
[4]Institute for Genetics, University of Cologne, Zülpicher Strasse 47a, Cologne 50674, Germany
[5]Max-Delbrück-Center for Molecular Medicine, Robert-Rössle-Strasse 10, Berlin-Buch 13125, Germany
[6]Humboldt-University Berlin, Institute of Biology, Invalidenstrasse 43, Berlin 10115, Germany
[7]Co-first authors
*Correspondence: antebi@age.mpg.de
http://dx.doi.org/10.1016/j.cell.2014.01.061

SUMMARY

Aging entails a progressive decline in protein homeostasis, which often leads to age-related diseases. The endoplasmic reticulum (ER) is the site of protein synthesis and maturation for secreted and membrane proteins. Correct folding of ER proteins requires covalent attachment of N-linked glycan oligosaccharides. Here, we report that increased synthesis of N-glycan precursors in the hexosamine pathway improves ER protein homeostasis and extends lifespan in *C. elegans*. Addition of the N-glycan precursor N-acetylglucosamine to the growth medium slows aging in wild-type animals and alleviates pathology of distinct neurotoxic disease models. Our data suggest that reduced aggregation of metastable proteins and lifespan extension depend on enhanced ER-associated protein degradation, proteasomal activity, and autophagy. Evidently, hexosamine pathway activation or N-acetylglucosamine supplementation induces distinct protein quality control mechanisms, which may allow therapeutic intervention against age-related and proteotoxic diseases.

INTRODUCTION

During aging, organisms undergo a decline in function and homeostasis, accompanied by reduced cellular, organ, and systemic performance. Nevertheless, aging can be modulated by environmental and genetic factors, and several mechanisms have been implicated in lifespan extension that are conserved from simple organisms to mammals (Kenyon, 2010). Among them are dietary restriction, reduced insulin/insulin-like growth factor 1 signaling (IIS), reduced mitochondrial respiration, and signals from the reproductive system (Kenyon, 2010), which trigger natural defense mechanisms that help stave off aging. Recent studies reveal that these pathways regulate diverse downstream processes, such as stress resistance, metabolism, quality control mechanisms, and immunity, to enhance life and health. However, the underlying proximal mechanisms of aging and the relative contribution of various defense mechanisms essential to longevity remain elusive.

Protein quality control mechanisms constitute a major regulatory output of longevity pathways, and aging and age-related diseases are associated with a decline in protein homeostasis. These processes are particularly evident in neurodegenerative diseases, which stem largely from a failure to properly handle protein misfolding, aggregation, and proteotoxic stress (Koga et al., 2011). The protein homeostasis network is required under normal conditions to support chaperone-assisted protein folding and to suppress protein aggregate formation (Balch et al., 2008). Different cellular compartments possess distinct proteotoxic stress response pathways; these include the cytosolic heat shock response, the mitochondrial unfolded protein response, and the endoplasmic reticulum (ER) unfolded protein response (UPR). In addition, autophagy, a turnover mechanism that degrades and recycles organelles and macromolecules, is induced during stress conditions such as starvation and thus plays a major role in protein quality control (Menzies et al., 2011). Notably, these pathways impinge on the aging process in *Caenorhabditis elegans* (Jia and Levine, 2010; Shore et al., 2012). Numerous long-lived mutant strains have the striking ability to maintain responsiveness to stress and to sustain protein homeostasis (Hsu et al., 2003; Morley and Morimoto, 2004; Zhou et al., 2011).

The ER is a major site of protein synthesis, lipid biosynthesis, and membrane biogenesis. All membrane and secreted proteins enter the ER and undergo a tightly regulated folding process, which includes the covalent attachment of complex sugars to

the amino group of asparagine residues in a process called N-glycosylation (Roth et al., 2010). N-glycans are structural components of secreted and cell surface proteins and also operate in ER protein folding quality control (Parodi, 2000). The presence of luminal unfolded proteins is an ER stress signal and triggers the UPR, a signaling cascade that results in attenuated translation and induced expression of ER-resident chaperones, such as heat shock protein 4 (HSP-4) (Walter and Ron, 2011). It is interesting to note that the remarkable longevity of animals with reduced IIS depends on proper ER quality control; in particular, the ER-UPR (Henis-Korenblit et al., 2010). Furthermore, the ER associated protein degradation (ERAD) machinery in combination with the ubiquitin-proteasome system removes ER luminal unfolded proteins for cytosolic degradation (Meusser et al., 2005). This multilayered protein quality assurance system suggests a significant requirement of ER protein homeostasis in healthy aging and longevity.

We reasoned that, if protein quality control mechanisms are indeed an important component of aging, then enhancing their effectiveness might improve health into old age and extend lifespan. We hypothesized that improved ER protein quality control itself promotes longevity. Using a forward genetic approach in *C. elegans*, we identified gain-of-function (gof) mutations in *gfat-1*, the key enzyme of the hexosamine pathway, as a novel regulator of protein quality control and longevity. GFAT-1 gain of function induces ERAD and autophagy and correlatively extends lifespan and ameliorates a broad spectrum of proteinopathies. These findings suggest novel therapeutic approaches to promote health and extend lifespan through endogenous molecule modulation of protein quality control.

RESULTS

gfat-1 gof Mutations Cause Resistance to ER Stress

To identify genes modulating aging through ER protein homeostasis, we performed a tunicamycin (TM) resistance screen in *C. elegans*. TM interferes with ER protein folding by inhibiting N-glycan synthesis and is a potent inducer of ER stress (Parodi, 2000). TM treatment of wild-type (WT) animals results in developmental retardation and lethality. We performed ethyl methanesulfonate (EMS) mutagenesis and selected mutants that completed development at the WT lethal dose of 10 μg/ml (Figure 1A). From more than 200,000 screened genomes, we isolated 358 TM-resistant mutant strains. Of those, 109 had an increased median lifespan (>15%). Through single-nucleotide polymorphism mapping and whole-genome sequencing, we identified three independent point mutations in a novel longevity gene F07A11.2, which encodes a putative glutamine-fructose 6-phosphate aminotransferase (called *gfat-1*). The *C. elegans* genome contains a homolog (F22B3.4), called *gfat-2*, that is 88.3% similar to *gfat-1* in amino acid sequence, but this gene was not found in our screen. We generated a transgenic *C. elegans* strain that carries additional WT *gfat-1* copies fused to cyan fluorescent protein (CFP), *gfat-1::cfp*. *gfat-1::cfp* was expressed most prominently in epidermal seam cells and the pharynx (Figure 1B). *gfat-1* is strikingly conserved across eukaryotes, with a 80% similarity between *H. sapiens* and *C. elegans* protein sequences (Figure 1C). Mammalian GFAT is the rate-limiting enzyme of the hexosamine pathway (HP), which synthesizes UDP-N-acetylglucosamine (UDP-GlcNAc) used as precursor for N- and O-glycans. (Figure 1D).

We observed normal development, pharyngeal pumping rates, and brood sizes in *gfat-1* mutants (Figures S1A and S1B available online). We tested TM resistance in the offspring of heterozygous *gfat-1* mutants and found that all three alleles conferred resistance in the heterozygous state (Figure S1C), indicating that the identified *gfat-1* alleles are dominant gof (gain-of-function) mutations. Accordingly, knockdown of the HP using RNAi against *gfat-1* and *gna-2* (catalyzing the second step of the HP) significantly reduced developmental TM resistance of *gfat-1* gof mutants (Figures S1D and S1E). Finally, we found that the *gfat-1::cfp* transgene increased TM resistance compared to controls expressing only CFP fused to the same 5′ and 3′ *gfat-1* regulatory elements (Figure 1E).

To elucidate whether GFAT-1 gof affects hexosamine metabolites, we used liquid chromatography mass spectrometry (LC-MS) and measured levels of endogenous UDP-N-acetylhexosamines (UDP-HexNAc), which represent the combined UDP-GlcNAc and UDP-N-acetylgalactosamine (UDP-GalNAc) pool. Consistent with gof, we found significantly elevated UDP-HexNAc levels in whole-worm lysates in all three *gfat-1* mutants by up to 10-fold (Figures 1F and 1G). No reduction in pyruvate or fructose 6-phosphate levels was observed (Figures S1F and S1G). TM resistance of the mutants also positively correlated with measured UDP-HexNAc levels (Figure S1H). This led us to ask whether exogenous supplementation of HP intermediates could alter TM toxicity. Indeed, WT animals successfully developed on TM plates with added GlcNAc or UDP-GlcNAc (Figures 1H and 1I), suggesting that dietary GlcNAc is utilized in the HP, as shown previously in cultured cells (Wellen et al., 2010). Additional data showed that GFAT-1 gof rendered animals resistant to TM-induced inhibition of N-glycosylation and subsequent UPR stress signaling (Figures S1I and S1P). In addition, we found that TM treatment induces *gfat-1* gene expression in WT animals (Figure S1Q). Together, these data demonstrate that elevation of cellular UDP-HexNAc levels through GFAT-1 gof or supplementation with UDP-GlcNAc or GlcNAc result in TM resistance.

Increased UDP-HexNAc Extends Lifespan

Given the altered ER stress response in our mutants, we asked if the novel *gfat-1* mutations affect lifespan. We found significant lifespan extension in all *gfat-1* gof mutants from 9% to 42%, which was completely dependent on *gfat-1* activity, as *gfat-1* knockdown abolished lifespan extension in *gfat-1* gof mutants, without having an effect on WT lifespan (Figure 2A; Figure S2A; Table S1). Likewise, transgenic overexpression of *gfat-1::cfp* resulted in similar lifespan extension (Figure 2B). Moreover, GlcNAc supplementation extended lifespan in WT animals up to a concentration of 10 mM, compared to the 10 mM D-arginine (D-Arg) osmolarity control (Figure 2C). By contrast, 25 mM GlcNAc failed to extend lifespan (Figure 2D), suggesting that an optimal GlcNAc concentration promotes beneficial effects. Thus, three independent lines of evidence indicate that elevated cellular UDP-HexNAc levels extend *C. elegans* survival.

Several longevity pathways in *C. elegans*, including reduced IIS pathway and germline removal, depend on the FOXO

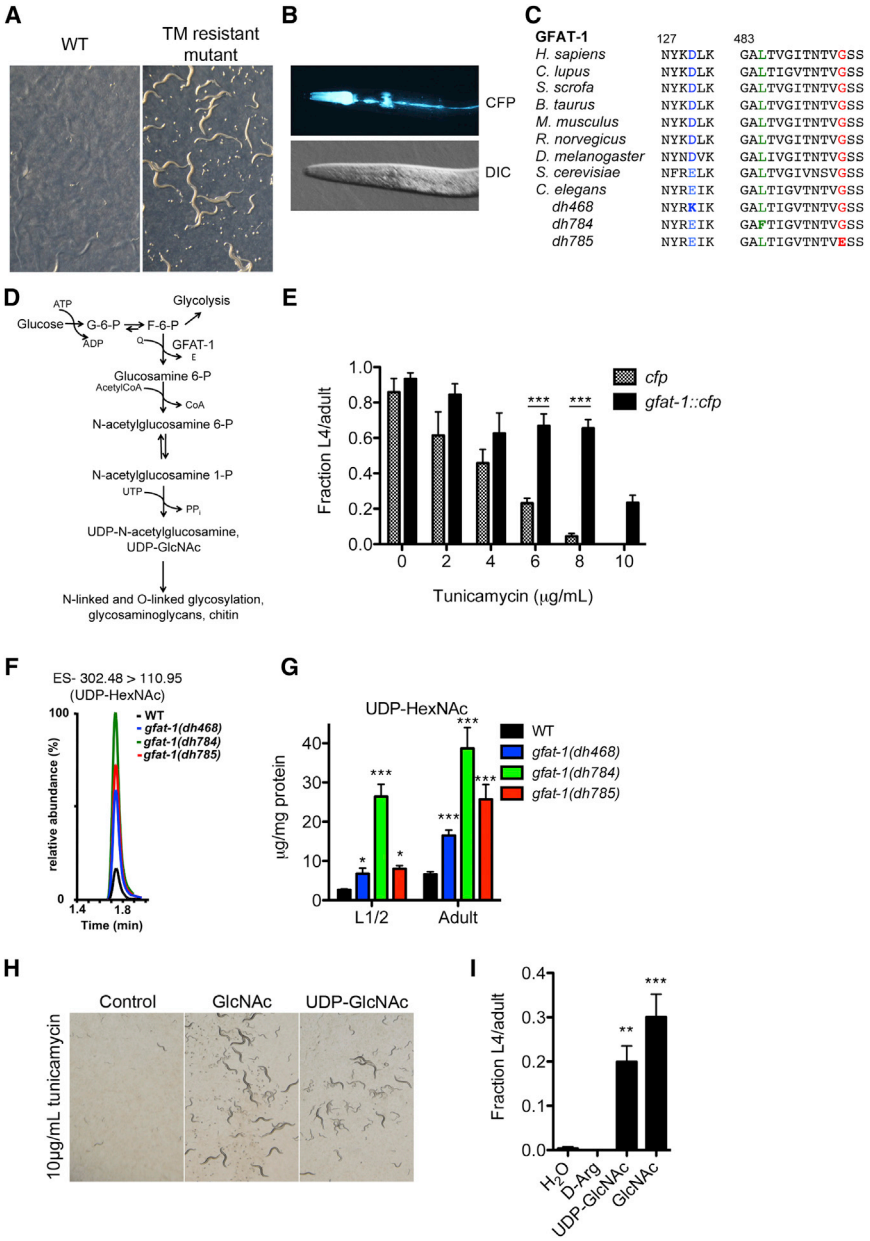

Figure 1. Developmental Tunicamycin Resistance Screen Identifies *gfat-1* gof Mutations

(A) Representative images of WT controls and tunicamycin (TM)-resistant *C. elegans* mutants after developmental screen for resistance to 10 μg/ml TM.

(B) Representative images of *dhEx941(Pgfat-1::gfat-1::cfp)* transgenic animal showing the GFAT-1 expression pattern in the head area of L4 animals. DIC, differential interference contrast.

(C) Multiple sequence alignment of *gfat-1* protein sequences surrounding the amino acid substitutions of alleles *dh468*, *dh784*, and *dh785*.

(D) The hexosamine pathway.

(E) Developmental TM resistance assay using transgenic animals expressing *cfp* or *gfat-1::cfp* fusion under *gfat-1* regulatory elements (n = 3). Results are presented as means ± SEM. ***p < 0.001.

(F) Representative LC/MS scans of adult *C. elegans* extracts.

(G) Quantitative LC/MS analysis of pooled L1/L2 larvae and adult animals for UDP-HexNAc levels in *dh468*, *dh784*, and *dh785* alleles of *gfat-1* (n = 8). Results are presented as means ± SEM. *p < 0.05 and ***p < 0.001 versus WT.

(H) Representative images of developmental TM resistance assay on control or 10 μg/ml TM plates with UV-killed OP50 bacteria, supplemented with 10 mM of indicated compounds.

(I) Quantification of the developmental TM resistance assay in (F). L4 or adult animals were counted 5 days after egg transfer to TM plates and displayed as a fraction of the number of eggs used (n = 6). **p < 0.01 and ***p < 0.001 versus D-Arg. Results are presented as means ± SEM.

See also Figure S1.

transcription factor DAF-16 (Kenyon, 2010). DAF-16 also mediates resistance to various types of cellular stress. We found that GFAT-1 gof-induced TM resistance was independent of DAF-16 and that DAF-16 target genes *sod-3*, *dod-3*, and *dod-8* remained unchanged (Figures S2B and S2C). Notably, GlcNAc supplementation and *gfat-1* gof mutation extended the lifespan of *daf-16(mgDf50)* and *daf-2(e1368)* mutants (Table S1), suggesting a mechanism, at least partially independent from DAF-16/FOXO and IIS longevity pathways. In addition, we detected no changes in the mRNA expression of representative cytosolic and mitochondrial chaperones (Figure S2D). No changes in UDP-HexNAc levels were observed in various long-lived animals, including those carrying mutations in genes affecting the IIS pathway (*daf-2*), gonadal outgrowth (*glp-1*), mitochondrial function (*isp-1*), dietary intake (*eat-2*), and protein translation (*ife-2*) (Figure 2E). Thus, known longevity pathways do not obviously activate the HP, implying a novel mechanism to extend lifespan. Furthermore, we found that UDP-HexNAc levels decreased with age, both in WT as in *gfat-1* gof mutants (Figure 2F).

In addition to N-glycosylation, which is specifically inhibited by TM, the HP gives rise to precursors used in O-glycosylation, which was previously implicated in *C. elegans* lifespan: O-GlcNAc transferase (*ogt-1*) loss-of-function mutants are short lived, while O-GlcNAcase (*oga-1*) mutants are modestly long lived (Rahman et al., 2010), revealing that enhanced O-glycosylation of client proteins is associated with longevity. However, neither *oga-1* nor *ogt-1* affected the *gfat-1* mutants' developmental TM resistance (Figure S2E) or lifespan (Table S1). Moreover, GlcNAc supplementation extended the lifespan of *ogt-1* mutants (Table S1). These results indicate that *ogt-1* mediated O-glycosylation does not play an appreciable role in developmental TM resistance or longevity of *gfat-1* gof mutants.

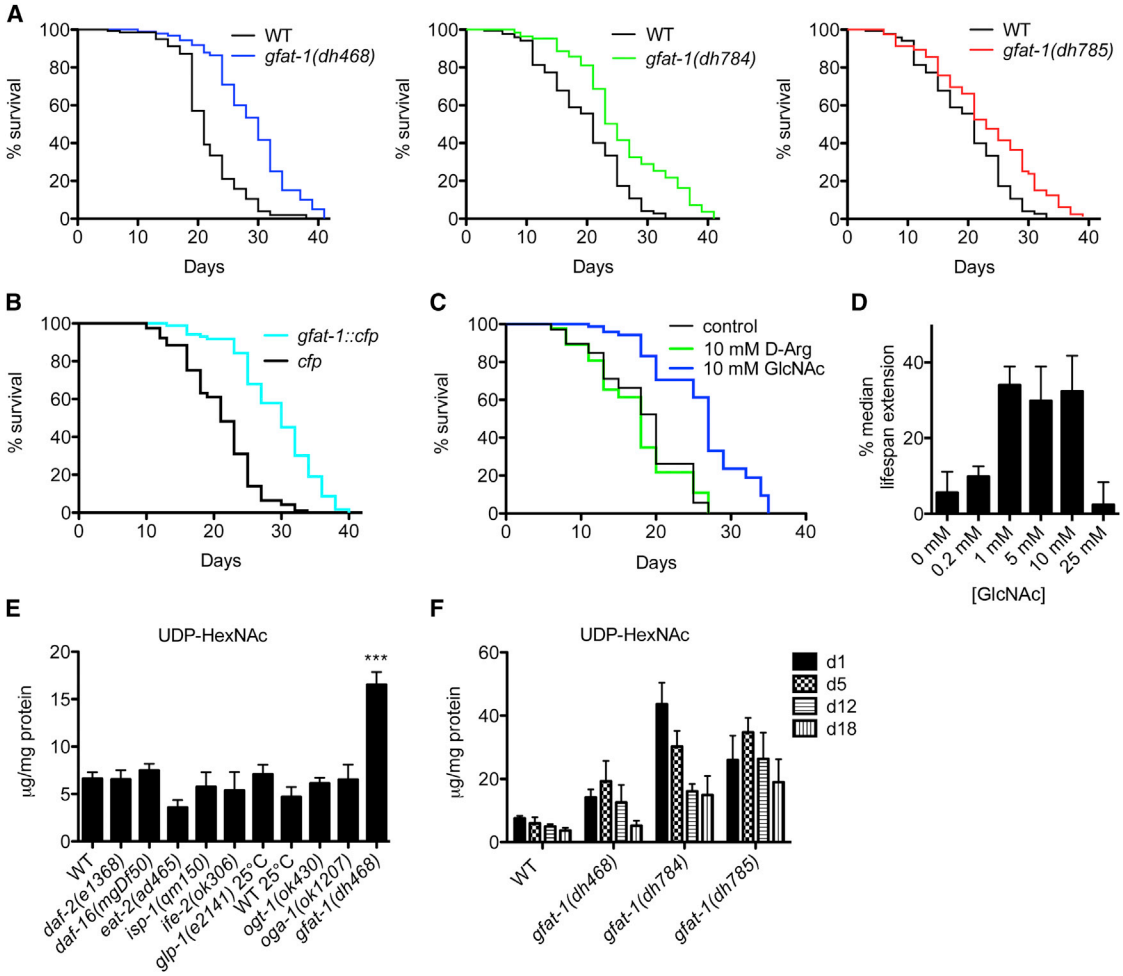

Figure 2. *gfat-1* gof or Supplementation with GlcNAc Extends *C. elegans* Lifespan

(A) Kaplan-Meier survival curves of *gfat-1* alleles *dh468*, *dh784*, and *dh785* show significant lifespan extensions (left: WT median lifespan = 21 days, and *gfat-1(dh468)* median lifespan = 30 days, $p < 0.0001$; middle: WT median lifespan = 21 days, and *gfat-1(dh784)* median lifespan = 25 days, $p < 0.0001$; right: WT median lifespan = 21 days, and *gfat-1(dh785)* median lifespan = 23 days, $p = 0.0004$).

(B) Lifespan assay using transgenic animals expressing *cfp* or *gfat-1::cfp* fusion under *gfat-1* regulatory elements (*Pgfat-1::cfp* median lifespan = 21 days, and *Pgfat-1::gfat-1::cfp* median lifespan = 30 days, $p < 0.0001$).

(C) Survival curves of WT animals on NGM plates supplemented with the indicated compounds. Animals were maintained on UV-killed OP50 *E. coli*. D-Arg was used as osmolarity control. (10 mM D-Arg median lifespan = 18 days, and 10 mM GlcNAc median lifespan = 27 days, $p < 0.0001$).

(D) Average median lifespan extension observed for the indicated GlcNAc concentrations (n = 3). Results are presented as means ± SEM.

(E) LC/MS analysis of indicated *C. elegans* mutants shows elevated UDP-HexNAc concentrations only in *gfat-1* mutants (n = 4–8). Results are presented as means ± SEM. ***$p < 0.001$ versus WT.

(F) Quantitative LC/MS analysis of UDP-HexNAc levels in WT animals and *gfat-1* gof mutant alleles at days 1, 5, 12, and 18 of adulthood (n = 3–6). Results are presented as means ± SEM.

See also Figure S2 and Table S1.

Increased HP Metabolite Levels Improve ER Protein Quality Control

We hypothesized that improved ER protein homeostasis might contribute to the observed lifespan extension and therefore asked whether elevation of HP metabolites causes changes in the protein folding milieu within the ER lumen. To this end, we made use of the neuroserpin homolog and folding sensor serpin 2 fused to yellow fluorescent protein (YFP) (SRP-2^{H302R}::YFP), which accumulates in the ER lumen due to a point mutation and whose aggregation is modulated by the heat shock response and the UPR (Schipanski et al., 2013). *srp-2::yfp* is expressed in the body wall muscles, and SRP-2^{H302R}::YFP aggregates were quantified in the head region. A time course analysis revealed an increase in SRP-2^{H302R}::YFP puncta from the L4 to adult stage and no further increase after the first day of adulthood in WT animals. At all measured time points, SRP-2^{H302R}::YFP accumulation was significantly reduced in *gfat-1* gof mutants (Figures 3A and 3B). Similarly, aggregation of SRP-2 was reduced in *gfat-1::cfp* transgenic animals (Figure 3C). Overall protein levels of SRP-2 were unchanged in

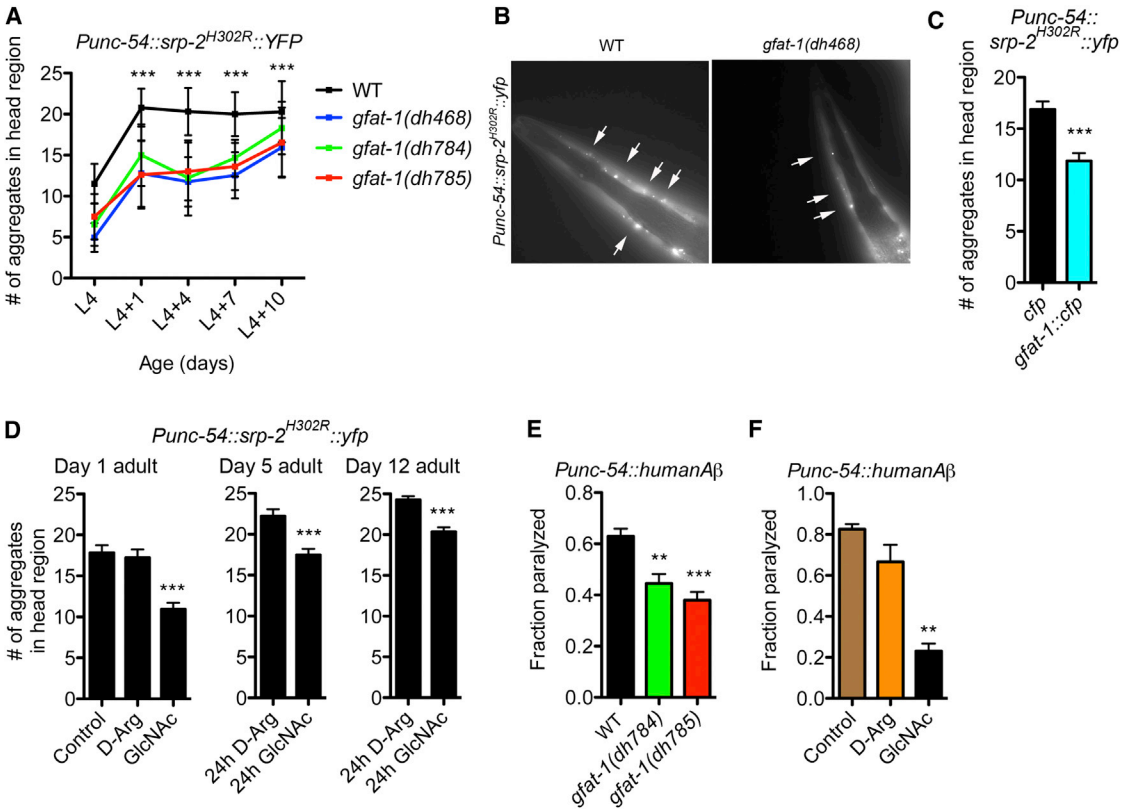

Figure 3. *gfat-1* gof or Supplementation with GlcNAc Improves ER Protein Quality Control

(A) Time course of SRP-2^{H302R}::YFP aggregation. Quantification was done in head region of ≥20 animals (data are means ± SD, representative result from n = 3 experiments; ***p < 0.001 versus *gfat-1*). Results are presented as means ± SEM.

(B) Representative fluorescent images of *Punc-54::srp-2^{H302R}::yfp* transgenic animals crossed to the indicated strains. Head regions are shown, and arrows point to SRP-2^{H302R}::YFP aggregates.

(C) Quantification of SRP-2^{H302R}::YFP in *cfp* and *gfat-1::cfp* transgenic animals (representative result from n = 3 experiments, t test). Results are presented as means ± SEM. ***p < 0.001 versus *cfp*.

(D) Quantification of SRP-2^{H302R}::YFP aggregates after exposure to the indicated compounds. Supplementation with compounds was done for the 24 hr prior to quantification (n = 3). Results are presented as means ± SEM. ***p < 0.001 versus D-Arg.

(E) Fraction of paralyzed *Punc-54::humanAβ* transgenic animals in WT or *gfat-1* gof mutant background at day 7 of adulthood (n = 4). Results are presented as means ± SEM. **p < 0.01 and ***p < 0.001 versus WT.

(F) *Punc-54::humanAβ* transgenic animals were treated with indicated compounds in a bath for 6 hr daily in the presence of UV-killed OP50 and otherwise maintained under standard culture conditions; fraction paralyzed worms was quantified at day 7 of adulthood. (n = 3; **p < 0.01 versus D-Arg). Results are presented as means ± SEM.

See also Figure S3.

both the *gfat-1* gof mutants and the *gfat-1::cfp* transgenic strain (Figures S3A and S3B), suggesting that reduced protein aggregation results from improved protein homeostasis. Additionally, the beneficial effects observed in *gfat-1* gof mutants arise from increased HP activity, since the decrease in SRP-2 aggregates was abolished upon *gfat-1* or *gna-2* knockdown (Figure S3C). Finally, GlcNAc treatment reduced SRP-2^{H302R}::YFP aggregation in young adults (Figure 3D).

Next, we tested if GlcNAc supplementation might clear already established SRP-2^{H302R}::YFP aggregates when provided at a later time during adulthood. Remarkably, 24 hr exposures to GlcNAc reduced SRP-2^{H302R}::YFP puncta at various adult time points until day 12 of adulthood (Figure 3D). Together, these data reveal that increased HP metabolite levels improve the ER's capacity not only to prevent accumulation of aggregated proteins but also to reverse aggregation. As an additional toxic aggregation-prone protein, we turned to animals expressing human ER-targeted Aβ42 peptide (Link, 1995; Link et al., 2001). These animals undergo progressive paralysis during adult aging due to Aβ toxicity. When crossed to *gfat-1* gof mutants or after GlcNAc treatment, transgenic Aβ animals showed significant motility improvements (Figures 3E and 3F).

To further explore ER function in *gfat-1* gof mutants, we investigated the role of N-glycosylation and UPR components in the aggregation dynamics of SRP-2^{H302R}::YFP. Inhibiting N-glycosylation by knockdown of oligosaccharyltransferase (OST) complex components suppressed the reduction of SRP-2^{H302R}::YFP puncta and lifespan extension found in *gfat-1* gof mutants (Figures S4A and S4B). These data suggest that N-glycosylation is required for improved protein homeostasis

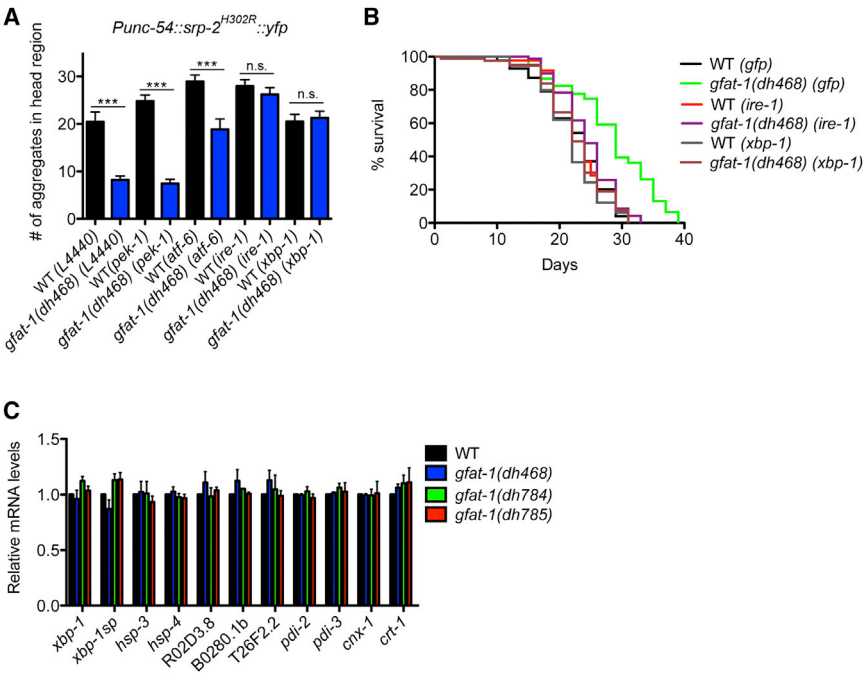

Figure 4. Role of the UPR in *gfat-1* gof Mutants

(A) SRP-2^{H302R}::YFP aggregate count in WT and *gfat-1(dh468)* mutants after RNAi-mediated knockdown of indicated UPR genes (n = 3). n.s., not significant. Results are presented as means ± SEM. ***p < 0.001.

(B) Representative survival demography of WT and *gfat-1(dh468)* animals treated with indicated RNAi targeting UPR genes. WT(*gfp*) median lifespan = 24 days, and *gfat-1(dh468)*(*gfp*) median lifespan = 29 days, p < 0.0001; WT(*ire-1*) median lifespan = 22 days, and *gfat-1(dh468)*(*ire-1*) median lifespan = 24 days, p < 0.005 versus *gfat-1(dh468)*(*gfp*); WT(*xbp-1*) median lifespan = 22 days, *gfat-1(dh468)*(*xbp-1*) median lifespan = 22 days, p < 0.001 versus *gfat-1(dh468)*(*gfp*).

(C) Relative mRNA levels of indicated UPR genes in WT animals and *gfat-1* mutants (n = 3). Results are presented as means ± SEM.

See also Figure S4 and Table S1.

and longevity in *gfat-1* gof mutants. Downregulation of the UPR pathway by RNAi against *ire-1* and *xbp-1* also increased SRP-2^{H302R}::YFP aggregates in *gfat-1* gof mutants (Figure 4A). Knockdown of *atf-6* only partly suppressed the beneficial effects from the *gfat-1* gof mutation, and *pek-1* knockdown had no effect. Correlatively, *gfat-1* gof longevity was completely dependent on *ire-1* and *xbp-1* (Figure 4B). These results suggest that specific branches of the UPR pathway coassist the improved protein homeostasis and longevity of *gfat-1* gof mutants. Unexpectedly, however, we found no changes in transcriptional regulation of known UPR target genes by qPCR (Figure 4C), including *hsp-4*, spliced *xbp-1*, and target genes of the ATF-6 and PEK-1 UPR branches (Shen et al., 2005). HSP-4 protein levels were slightly increased without reaching statistical significance, and CNX-1 protein levels were unchanged (Figures S4C and S4D), suggesting that a functional UPR is required but not activated in *gfat-1* gof mutants.

We were surprised to find no evidence for UPR induction; thus, we hypothesized that ERAD activity might be induced. ERAD client proteins are retrotranslocated from the ER lumen to the cytosol before proteasomal degradation. The SEL-11/HRD1 ubiquitin ligase complex controls this translocation and ubiquitin-dependent degradation process (Bordallo et al., 1998), in conjunction with the ER membrane glycoprotein SEL-1/HRD3 that serves as a cofactor (Hampton et al., 1996). We found a 2-fold increased expression of SEL-1 protein in all three *gfat-1* gof mutants using western blot analysis of worm lysates (Figures 5A and 5B), without accompanying changes in mRNA levels (Figure S5A). Similarly, *gfat-1::cfp* transgenic animals and WT animals supplemented with GlcNAc showed slightly elevated levels of SEL-1 (Figures S5B and S5C). We next tested the role of ERAD in SRP-2^{H302R}::YFP aggregation and lifespan extension of *gfat-1* gof mutants. RNAi experiments identified a strict requirement for *sel-1* and *sel-11*, as knockdown suppressed the *gfat-1* mutants' ER luminal aggregation and longevity phenotypes (Figures 5C and 5D). Strikingly, a *sel-1::gfp* transgenic strain was long lived compared to WT controls (Figure 5E), suggesting the *gfat-1* gof induced longevity could arise in part from increased *sel-1* expression and activity.

Given the apparent involvement of the ERAD machinery, we tested proteasome activity. We observed a mild yet significant increase in chymotrypsin-like proteasome activity, as measured by turnover of an LLVY-tagged fluorescent substrate, in all *gfat-1* gof alleles (Figures 5F and 5G). Additionally, *gfat-1(dh785)* showed a significant increase in trypsin-like activity (Figure S5D). GlcNAc supplementation stimulated both activities in WT animals, although the trypsin-like activity did not reach significance (Figure 5H; Figure S5E). If the *gfat-1* gof mutants enhance proteasome activity, then they might exhibit resistance to bortezomib, a known proteasome inhibitor. Indeed, in *gfat-1* gof mutants we observed significantly elevated resistance to 30 μM bortezomib compared to WT controls (Figure S5F). RNAi knockdown of proteasome subunit genes *rpn-6* and *rpn-8* abrogated lifespan extension of *gfat-1* but also shortened WT lifespan (Table S1). Together, increased expression of SEL-1 and enhanced proteasome activity suggest that improved ER protein homeostasis in *gfat-1* gof mutants is linked to longevity and enhanced proteolytic capacity.

Elevated HP Metabolite Levels Induce Autophagy

Another quality control mechanism that contributes to the turnover of aggregation prone proteins is autophagy, a cellular degradation pathway known to play a role in protein and organellar homeostasis (Menzies et al., 2011). Recent data also suggest that the hexosamine metabolite glucosamine can induce autophagy in cell culture experiments (Shintani et al., 2010), but the influence of other such metabolites in a multicellular organism is unknown. During autophagosome formation, the nematode microtubule-associated protein light chain 3

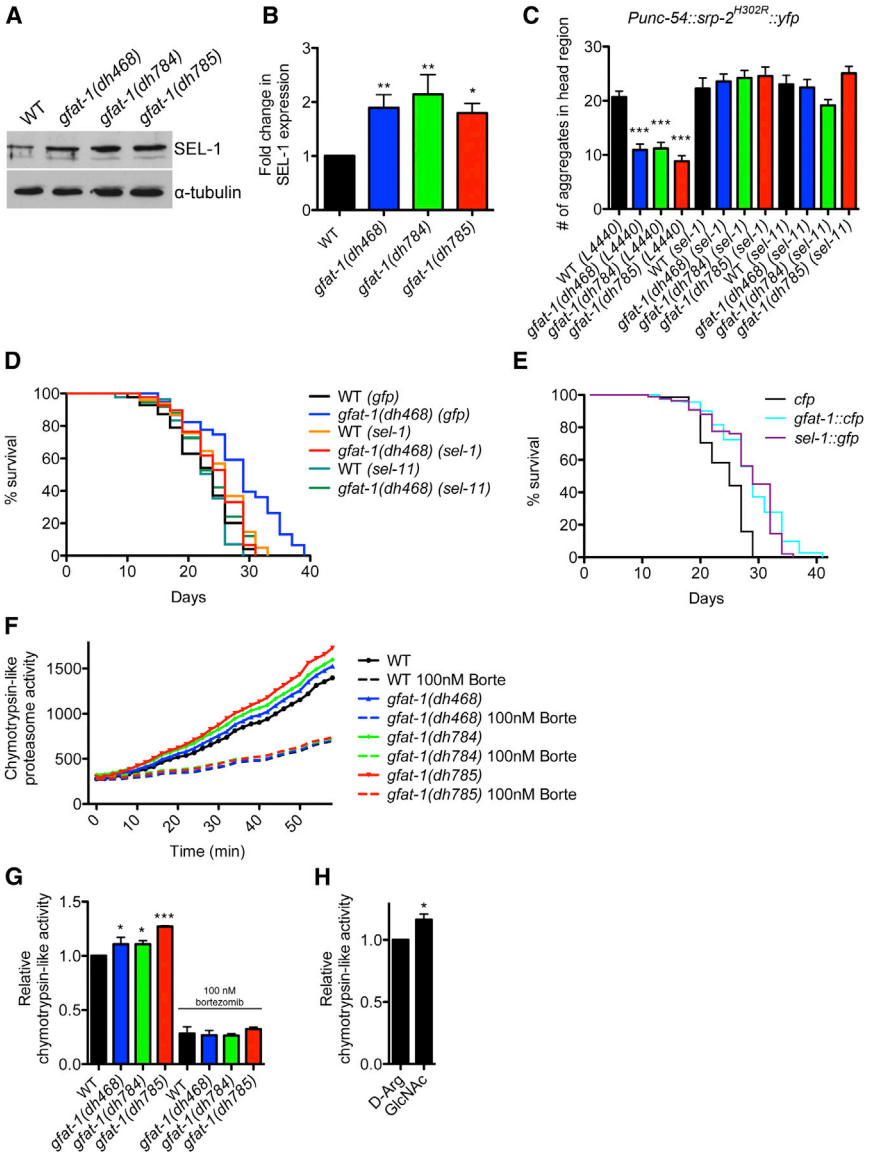

Figure 5. *gfat-1* gof Mutants Show Increased ERAD Activity

(A) Representative western blot from L4 animals from indicated genotypes detecting SEL-1 and α-tubulin.

(B) Analysis of SEL-1 western blots from n = 3 independent experiments. SEL-1 levels were normalized to α-tubulin. Results are presented as means ± SEM. *p < 0.05 and **p < 0.01 versus WT.

(C) SRP-2^{H302R}::YFP aggregation in WT and *gfat-1* gof mutants treated with RNAi targeting ERAD genes *sel-1* and *sel-11* (n = 3). Results are presented as means ± SEM. ***p < 0.001 versus WT.

(D) Lifespan analysis of WT and *gfat-1(dh468)* animals treated with indicated RNAi targeting ERAD gene expression. WT(*gfp*) median lifespan = 24 days, and *gfat-1(dh468)*(*gfp*) median lifespan = 29 days, p < 0.0001; WT(*sel-1*) median lifespan = 22 days, and *gfat-1(dh468)*(*sel-1*) median lifespan = 22 days, p < 0.005 versus *gfat-1(dh468)*(*gfp*); WT(*sel-11*) median lifespan = 24 days, and *gfat-1(dh468)*(*sel-11*) median lifespan = 24 days, p < 0.005 versus *gfat-1(dh468)*(*gfp*).

(E) Representative lifespan curves of *Pgfat-1::cfp*, *Pgfat-1::gfat-1::cfp*, and *sel-1::gfp* (*Pgfat-1::cfp* median lifespan = 25 days versus *Pgfat-1::gfat-1::cfp* median lifespan = 29 days, p < 0.005, and versus *sel-1::gfp* median lifespan = 29 days, p < 0.005).

(F) Representative example of chymotrypsin-like proteasome activity assay measuring LLVY-AMC turnover at 25°C with in lysates of L4 larvae. Treatment with the proteasome inhibitor bortezomib served as a negative control.

(G) Relative chymotrypsin-like activity from n = 4 experiments with animals of indicated genotypes. Results are presented as means ± SEM. *p < 0.05 and ***p < 0.001 versus WT.

(H) Relative chymotrypsin-like activity from n = 4 experiments with WT animals and indicated treatments. Results are presented as means ± SEM. *p < 0.05 versus D-Arg.

See also Figure S5 and Table S1.

(LC3) homolog LGG-1 condenses into puncta, reflecting the activity of autophagic processes (Meléndez et al., 2003). When we quantified LGG-1::GFP foci in epidermal seam cells, we observed a 60%–70% increase of LGG-1::GFP foci in the *gfat-1* gof mutants relative to WT (Figure 6A; Figure S6A) and saw a similar increase upon GlcNAc supplementation (Figure S6B). This enhancement was due to increased HP activity since *gfat-1* and *gna-2* RNAi reduced LGG-1::GFP puncta formation (Figure S6C). Concomitantly, we detected an increase in the lipidated form of LGG-1::GFP in *gfat-1* gof mutants and after GlcNAc treatment (Figures 6B and 6C; Figures S6D–S6F), suggesting that autophagic activity was enhanced. To confirm this idea, we quantified turnover of p62, a physiological substrate that is selectively removed by autophagy (Tian et al., 2010). We observed a reduction in p62 foci in the posterior pharyngeal bulb in GFAT-1 gof animals (Figure 6D). No changes in the mRNA expression of autophagy genes were detected (Figure 6E), suggesting that autophagy is induced posttranscriptionally.

Since autophagy was induced, we tested if improved ER protein homeostasis and lifespan extension of *gfat-1* gof mutants depended on autophagy. We found that inhibition of autophagy by RNAi-mediated knockdown of the gene *atg-18* specifically increased SRP-2^{H302R}::YFP aggregation in *gfat-1* gof mutants (Figure 6F). Moreover, *atg-18* RNAi shortened lifespan in *gfat-1* gof mutants but not in WT controls (Figure 6G). Taken together, *gfat-1* gof mutations induce autophagy, which supports ER protein homeostasis and lifespan extension.

Increased HP Activity Alleviates Proteotoxicity in *C. elegans* Disease Models

Given that HP metabolites enhanced both the proteasome and autophagy, we wondered whether observed changes in protein homeostasis might go beyond the ER. We used

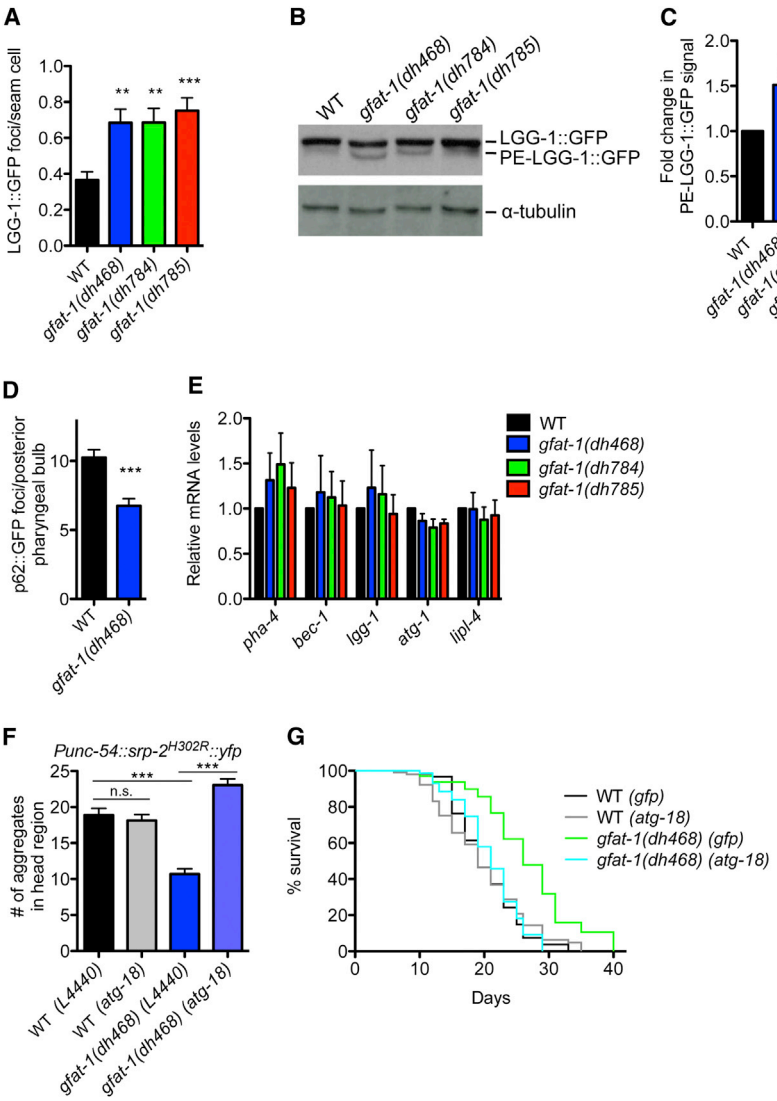

Figure 6. *gfat-1* gof Extends Lifespan via Induction of Autophagy

(A) Average number of LGG-1:GFP foci per seam cell of L3 larvae in indicated genotypes shows elevated autophagosome formation in *gfat-1* gof mutants. Results are presented as means ± SEM. $^{**}p < 0.01$ and $^{***}p < 0.001$ versus WT.

(B) Representative western blot using anti-GFP antibodies to detect LGG-1::GFP fusion protein in L4 animals shows increase of phosphatidylethanolamine-LGG-1::GFP in *gfat-1* gof mutants.

(C) Analysis of LGG-1::GFP western blots as in (B) from n = 6 experiments. PE-LGG-1::GFP levels were normalized to α-tubulin. Results are presented as mean ± SEM. $^{*}p < 0.05$ versus WT.

(D) Average number of p62::GFP foci per posterior pharyngeal bulb of L4 larvae in ≥ 15 WT and *gfat-1(dh468)* animals (t test, representative result of n = 3 experiments). Results are presented as means ± SEM. $^{***}p < 0.001$ versus WT.

(E) Quantitative real-time PCR measurements of autophagy genes in L4 animals from indicated genotypes (n = 5). Results are presented as means ± SEM.

(F) Quantification of SRP-2^{H302R}::YFP aggregates in L4 animals after developmental exposure to *atg-18* RNAi or L4440 empty vector control (representative result of n = 3 experiments). Results are presented as means ± SEM. n.s., not significant. $^{***}p < 0.001$ versus WT or *gfat-1(dh468)*, respectively as indicated.

(G) Kaplan-Meier survival curves of N2 and *gfat-1(dh468)* animals exposed to indicated RNAi shows significant lifespan extension in *gfat-1(dh468)* animals on control RNAi but not after *atg-18* RNAi treatment. WT(*gfp*) median lifespan = 19 days, and *gfat-1(dh468)*(*gfp*) median lifespan = 26 days, $p < 0.0001$; WT(*atg-18*) median lifespan = 19 days, and *gfat-1(dh468)*(*atg-18*) median lifespan = 21 days, $p < 0.0001$ versus *gfat-1(dh468)*(*gfp*).

See also Figure S6 and Table S1.

additional models of protein aggregation, including polyglutamine (polyQ40) repeats and α-synuclein, which are not targeted to the ER. PolyQ repeats are found in aggregation-prone proteins such as Huntingtin, implicated in Huntington's disease, whereas α-synuclein is associated with Parkinson's and Alzheimer's diseases (Douglas and Dillin, 2010; Johnson, 2000). Because polyQ40 and α-synuclein transgenic animals express the ectopic toxic protein species in muscle cells, we used motility as a readout for toxicity by counting the number of bodybends in liquid. We found significant motor function improvements in both proteotoxic disease models on a 6-day treatment initiated from young adulthood for 6 hr/day with 10 mM GlcNAc supplemented in liquid (Figures 7A and 7B). A role of the HP in protection from proteotoxicity was further corroborated by improved motor function in *gfat-1* gof mutants carrying the same transgenes (Figures 7C and 7D). As with SRP-2 expression, overall abundance of Q40::GFP and α-synuclein::GFP was not reduced in the *gfat-1* gof mutants (Figures S7A and S7B). Knocking down *gfat-1* or *gna-2* abolished the improvement without changing WT motility (Figures S7C and S7D). In addition, *atg-18* RNAi, as well as knockdown of *sel-1* and *sel-11* suppressed the beneficial effects on motility in both α-synuclein and polyQ40 transgenic animals (Figures 7C–7F). These data indicate that the protective effects in *gfat-1* gof mutants are not limited to the ER and that they depend on HP activity, ERAD, and autophagy.

Furthermore, we wanted to see if the HP pathway could influence toxic phenotypes in the nervous system. We therefore examined animals expressing α-synuclein under the *dat-1* promoter in dopaminergic neurons. We found improved motility in this neuronal proteotoxicity model in *gfat-1* gof mutants (Figure 7G). Together, these data show that HP metabolites induce broad-spectrum protection against proteotoxicity in various tissues and cellular compartments.

DISCUSSION

The current study provides a previously unknown link between endogenous hexosamine metabolites and cellular protein quality

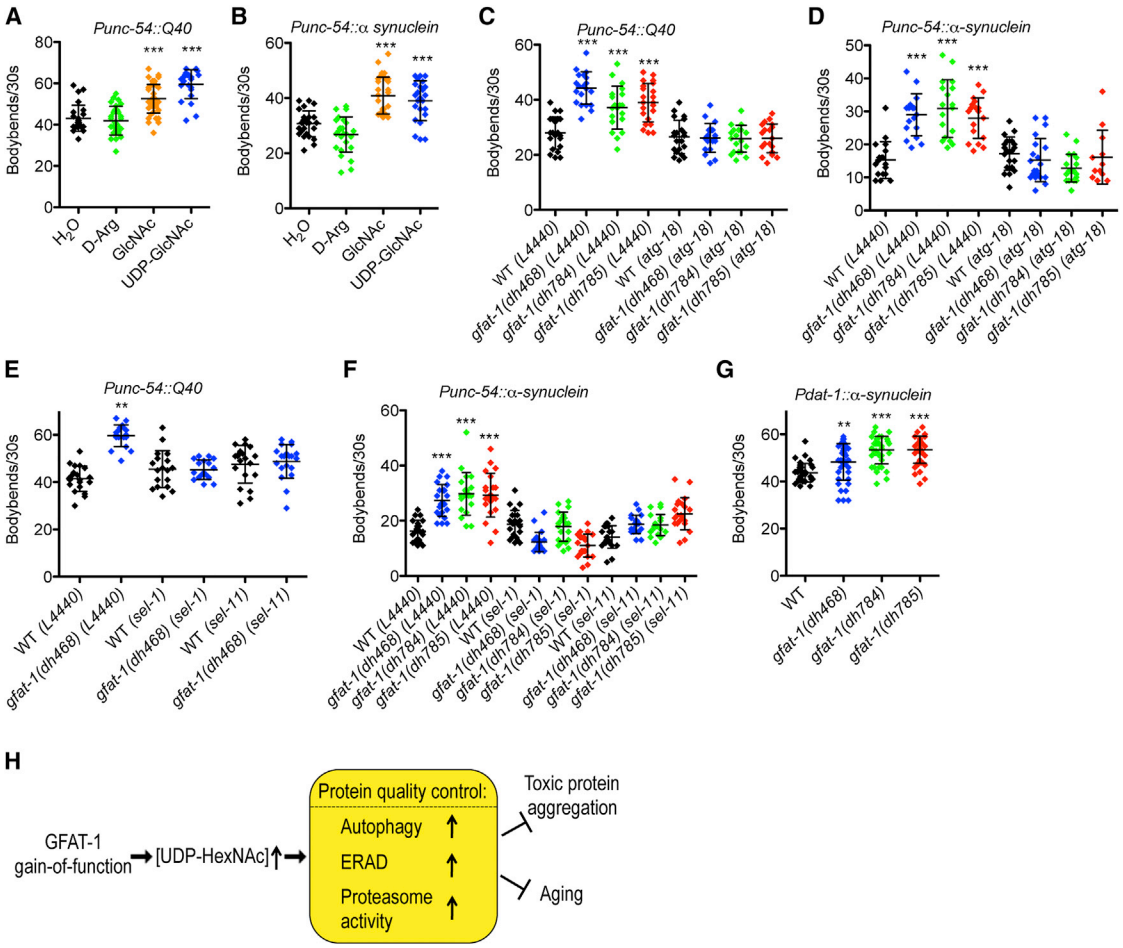

Figure 7. GlcNAc Supplementation or *gfat-1* gof Alleviate Multiple Forms of Proteotoxicity

(A and B) Motility assays using 7-day-old animals with *Punc-54*-driven muscle-specific expression of (A) polyQ40-YFP fusion protein and (B) α-synuclein-GFP reveal significant improvement in motor function when treated with UDP-GlcNAc or GlcNAc.

(C and D) Motility assay using (C) *Punc-54::polyQ40* and (D) *Punc-54::α-synuclein* transgenic animals at day 7 of adulthood after exposure to indicated RNAi starting from day 1 of adulthood.

(E and F) Motility assay using (E) *Punc-54::polyQ40* and (F) *Punc-54::α-synuclein* transgenic animals at day 7 of adulthood after exposure to indicated RNAi starting from day 1 of adulthood.

(G) Motility assay in indicated *gfat-1* mutants with transgenic expression of α-synuclein specifically in dopaminergic neurons.

All data are means ± SD, n = 3. **p < 0.01 and ***p < 0.001 versus D-Arg or WT controls.

(H) Model. GFAT-1 gof elevates hexosamine pathway activity and/or UDP-HexNAc availability. This activates the protein quality control mechanisms autophagy, ERAD, and the proteasome, which in concert results in suppression of ER and cytoplasmic proteotoxicity and in lifespan extension.

See also Figure S7.

control, leading to improved protein homeostasis and lifespan extension. Using *gfat-1* gof mutations and activation of the HP pathway, we demonstrate that elevated levels of the endogenous metabolite UDP-GlcNAc extend longevity and ameliorate various proteinopathies. Lifespan extension induced by GlcNAc or *gfat-1* gof required multiple aspects of ER function, including N-glycosylation, ERAD, and UPR signaling. It is important to note that GlcNAc supplementation or GFAT-1 gof alleviated—and, in some cases, reversed—proteotoxicity in models of neurodegenerative disease in diverse tissues and cellular compartments. This suggests broad-spectrum improvements in protein quality control. Our data indicate that such improved homeostasis stems largely from posttranscriptional enhancement of ERAD function, proteasome activity, and autophagy, suggesting coordinate regulation of these processes through interactions between metabolites and proteins. Moreover, elevated levels of UDP-HexNAc are not seen in several major models of longevity such as reduced insulin signaling, mitochondrial function, gonadal longevity, or dietary restriction, suggesting that *gfat-1* gof mutation invokes a novel mechanism to prolong life. These results point to new strategies to combat proteotoxic diseases through endogenous small molecule metabolites.

Aging and ER Function

Several studies have previously linked ER function and its stress response pathways to effects on health and lifespan (Brown and

Naidoo, 2012; Parodi, 2000). Many age-related diseases and conditions, including diabetes, chronic inflammation, heart disease, and neurodegenerative diseases, show perturbation in the ER stress response (Cao and Kaufman, 2013; Ozcan and Tabas, 2012; Walter and Ron, 2011). Moreover, components of UPR signaling are required for lifespan extension of *C. elegans daf-2*/Insulin receptor mutants (Henis-Korenblit et al., 2010). More recently, constitutive activity of the XBP-1 transcription factor has been shown to work cell nonautonomously to stimulate longevity, demonstrating that UPR activation is sufficient for lifespan extension (Taylor and Dillin, 2013). The UPR is thought to stimulate ERAD and autophagy through various proposed mechanisms (Qin et al., 2010; Shen et al., 2005; Yorimitsu and Klionsky, 2007; Zhao et al., 2013). Although *gfat-1* gof mutants require basal UPR for lifespan extension and aggregate removal, it is surprising that we found no evidence for transcriptional induction of this pathway, as measured by *xbp-1* splicing and mRNA levels of downstream target genes such as *hsp-4* (Figure 4). Similarly we found that, while *gfat-1* gof-induced longevity depended on components of ERAD, autophagy, and N-glycosylation, it did not give rise to obvious transcriptional changes; nor did we see changes in mRNA levels of genes involved in other stress pathways such as mitochondrial UPR genes (*hsp-6*, *hsp-60*) or cytosolic heat shock response genes (*hsp-16.2*, *hsp-70*) (Figure S2D). Preliminary global transcriptome analysis of *gfat-1* mutants further revealed virtually no changes in mRNA levels (data not shown). GFAT-1 gof instead appears to stimulate autophagic vesicle formation, ERAD protein expression, and proteasome activity, although other aspects of protein homeostasis might also be affected. These observations highlight a posttranscriptional and proximal mechanism for longevity that affects metabolite levels and their interaction with client proteins.

Links between Hexosamine Metabolites, ER Physiology, and Autophagy

How might hexosamine metabolites influence ERAD, proteasome activity, and autophagy? One possibility is that phenotypes result from broad changes in the secretory apparatus, presumably by modulation of N-glycosylation. However, we failed to observe global changes in steady-state protein glycosylation as measured by N-glycan labeling with concanavalin A (Figures S1I and S1J). Another possibility is that specific secretory proteins may be affected. Indeed, the observation that increased UDP-GlcNAc results in increased expression of SEL-1 protein, involved in ERAD, may provide an important hint. Conceivably, elevated UDP-GlcNAc stimulates the covalent N-glycosylation of SEL-1 and other ERAD components, thereby affecting their activity and/or stability. Consistent with this idea, increased gene dose of *sel-1* is sufficient to extend lifespan. In addition, we detected a dependence of *gfat-1*-induced aggregate clearance and longevity on components of the N-glycosylation machinery (Figure S4). It is noteworthy that Hrd3p, the yeast homolog of SEL-1, is a glycoprotein itself (Saito et al., 1999) that functions in a complex with the Hrd1p/SEL-11 ubiquitin ligase and has been shown to autoregulate its own activity (Plemper et al., 1999). Presumably, elevated SEL-1 enhances ubiquitination, ERAD, and proteasome activity to improve protein degradation. It is also possible that hexosamine metabolites noncovalently affect interacting proteins. Future experiments should clarify the possible mechanisms at work.

How might ERAD and autophagy be linked? In certain pathological serpinopathy models, ERAD has been shown to be stimulated concomitantly with autophagy, resembling our observations with GFAT-1 gof (Kroeger et al., 2009) (Figures 5 and 6). However, in our mutants, we saw no overt evidence for endogenous protein misfolding stress; animals had normal developmental timing and brood sizes and demonstrated better handling of misfolded proteins. Another view is that organellar homeostasis within the ER may require intimate coordination of these processes. Autophagosomes form at ER-mitochondria contact sites; thus, ER membranes might be an origin for autophagic vesicle formation (Hamasaki et al., 2013). Such sites may be used to initiate normal macroautophagy. Alternately, they may facilitate so-called ERAD tuning, in which ERAD components are selectively removed from the ER to dampen the degradation response. During ERAD tuning, the unlipidated form of LC3 physically associates with SEL-1 to mediate this process (Bernasconi et al., 2012). In *gfat-1* gof mutants, however, we observed an increase in the lipidated form of LC-3, consistent with canonical autophagy (Figure 6).

Several other small molecule metabolites have been shown to stimulate autophagy, including spermidine, trehalose, and others (Eisenberg et al., 2009; Honda et al., 2010). It is unclear if they work in concert with GlcNAc or affect a parallel pathway. It is striking that a single endogenous metabolite such as GlcNAc can stimulate both ER quality control and autophagy, suggesting a potential role as a signaling molecule.

These studies also provide strong evidence that enhanced protein homeostasis promotes health and increases life span. It will be interesting to see if these observations extend to mammals and can lead to new strategies to combat proteotoxic diseases.

EXPERIMENTAL PROCEDURES

C. elegans Strains and Culture

Nematodes were cultured at 20°C on nematode growth medium (NGM) agar plates with the *E. coli* strain OP50, unless indicated otherwise (Brenner, 1974). For strains and details of the TM resistance screen, see the Extended Experimental Procedures. For the genetic dominance test, *gfat-1* mutant animals were crossed with N2 males, and TM resistance was scored in the F2 offspring of F1 heterozygous animals.

Mutant Mapping and Sequence Analysis

Rapid single nucleotide polymorphism mapping was conducted as previously described (Davis et al., 2005). Genomic DNA was prepared using the QIAGEN Gentra Puregene Kit. Whole-genome sequencing was conducted on the Illumina HiSeq2000 platform. Sequencing outputs were analyzed using the MAQGene pipeline (Bigelow et al., 2009). Paired-end reads (100 base pairs long) were used; the average coverage was larger than 20-fold.

qRT-PCR

See the Extended Experimental Procedures for quantitative RT-PCR (qRT-PCR). Primers are listed in Table S2.

RNAi

RNAi experiments were performed as described elsewhere (Kamath and Ahringer, 2003; Rual et al., 2004). Synchronized eggs were put on corresponding RNAi plates containing IPTG and ampicillin. *gfp* (GFP::L4440) RNAi or empty

vector (L4440) were used as a nontargeting control. RNAi clones used are listed in Table S3.

Lifespan Assays

Adult lifespan analyses were performed at 20°C on *E. coli* OP50; the young adult stage was defined as as day 0. One hundred to 150 animals were used per condition and scored every day or every second day. The secondary longevity screen after TM selection was conducted on 50 μM FUDR plates. Animals in all RNAi lifespan assays were treated with RNAi from young adults (L4 + 1 day) and kept on RNAi bacteria-containing plates throughout the experiment. Worms that had undergone internal hatching, vulval bursting, or crawling off the plates were censored. Throughout the experiment, strain and/or treatment was unknown to researcher. In some experiments, all plates were numbered and randomly mixed. In both cases, data were assembled on completion of the experiment. Statistical analyses were performed with the Mantel-Cox log rank method in Excel (Microsoft).

Paralysis and Motility Assays

Paralysis of *dvIs2[pCL12(Punc-54::human Abeta peptide 1-42 minigene; pRF4(rol-6(su1006)))]* animals was scored daily by prodding animals at head and tail with a wire on NGM plates. Animals that were alive but unable to roll were scored as paralyzed. Motility assays were carried out by transferring animals to M9 and counting body bends over a 30 s interval.

Compound Feeding and Developmental TM Resistance Assay

For developmental TM resistance assays with GlcNAc and UDP-GlcNAc (Sigma), UV-radiation-killed bacteria were transferred to plates containing 10 μg/ml tunicamycin. Compounds were then added to the plate surface, resulting in a 10 mM compound concentration in the plates. Fifty to eighty synchronized WT (N2) eggs per condition were added to the plates, and development to L4 or adult stage was scored after 4 and 5 days. For adult exposure experiments for lifespan analyses with D-Arg or GlcNAc, compounds were mixed with the NGM agar to a final concentration of 10 mM unless otherwise noted, and UV-killed OP50 bacteria were added on the plates. For motility assays, adult exposure experiments were carried out by maintaining animals on normal NGM agar plates with a daily 6 hr treatment in S-basal media supplemented with UV-killed OP50 bacteria and the indicated compounds.

LC/Tandem MS Analysis

See the Extended Experimental Procedures.

Western Blotting

Twenty-five L4 animals were suspended in Laemmli lysis buffer under reducing conditions. Proteins were separated by reducing SDS-PAGE and transferred to PVDF membranes. Membranes were then incubated with specific antibodies to GFP (Clontech), α-tubulin (Sigma), and SEL-1 (produced in the Sommer laboratory).

Plasmid Construction and Transgenes

See the Extended Experimental Procedures.

Autophagy Quantification

Autophagosomes were scored as reported previously (Lapierre et al., 2011). Fifteen to 25 transgenic *lgg-1::gfp* animals per condition where whole mounted, and foci were counted using 100× magnification on a Zeiss Axio Imager.Z1 microscope in the seam cells of L3 larvae. For quantification of p62::GFP puncta, 10–20 L4 larvae were whole mounted, and GFP foci in the posterior pharyngeal bulb were quantified. For quantification, we used 100× magnification on a Leica TCS SP5-X confocal microscope.

Quantification of SRP-2^{H302R}::YFP Aggregation

SRP-2^{H302R}::YFP puncta were scored in transgenic animals in WT or *gfat-1* gof backgrounds. At least 20 animals were whole mounted per experiment, and GFP puncta were counted using a Zeiss Axio Imager.Z1. For clarity of imaging, only the aggregates in the animals' head regions were scored.

Proteasome Activity Assay

Proteasome chymotryptic and tryptic activity was assayed according to standard procedures (Fredriksson et al., 2012) as the rate of hydrolysis of the fluorogenic peptide suc-LLVY-AMC (Sigma) or ac-RLR-AMC (Enzo), respectively. Extracts were prepared in 25 mM Tris HCl, pH 7.5, using a dounce homogenizer. Protein (20 μg) was incubated with 12.5 μM suc-LLVY-AMC or ac-RLR-AMC in a total volume of 200 μl. AMC fluorescence was measured using 355 nm excitation and 460 nm emission filters with free AMC (Sigma) as standard every 2 min for 1 hr at 25°C.

Statistical Analysis

Results are presented as means ± SEM unless noted otherwise. For each experiment, at least three biological replicates were carried out, and genotypes were blinded during analysis. Statistical tests were performed using one-way ANOVA with a Bonferroni posttest, unless otherwise noted, with GraphPad Prism (GraphPad software). Chi-square two-tailed p values were calculated with GraphPad QuickCalcs. Significance levels are *$p < 0.05$, **$p < 0.01$, and ***$p < 0.001$ versus WT control unless otherwise noted.

SUPPLEMENTAL INFORMATION

Supplemental Information includes Extended Experimental Procedures, seven figures, and three tables and can be found with this article online at http://dx.doi.org/10.1016/j.cell.2014.01.061.

AUTHOR CONTRIBUTIONS

N.J.S. and M.S.D. performed the TM resistance assay and lifespan analyses. M.S.D. did western blotting, LC/MS analysis, proteasome activity, and bortezomib resistance. N.J.S. did autophagy, ERAD, lifespan, and motility assays. M.S.D. and N.J.S. did the data analysis. A.G. conducted the SEL-1 western blotting with an antibody made by E.J. and T.S. Y.H. performed all LC/MS experiments. R.B. assisted in survival analysis, qPCR experiments, and preparation of samples for LC/MS. M.S.D., N.J.S., T.H., and A.A. designed the experiments. M.S.D., N.J.S., and A.A. wrote the manuscript.

ACKNOWLEDGMENTS

We thank the Caenorhabditis Genetics Center for strains. We also thank Dr. Claudia Knief and Dr. Richard Reinhardt from the Max Planck Genome Centre Cologne for whole-genome sequencing and Dr. Assa Yeroslaviz for support with bioinformatic analyses. This work was supported by an EMBO fellowship and a Marie-Curie Career Integration Grant (M.S.D.); by the Max Planck Society, BMBF/Sybacol, and Deutsche Forschungsgemeinschaft (DFG)/CECAD (A.A.); by grants from the DFG, the DIP8 grant 2014376, CECAD FOR885, KFO286, and SFB635 (T.H.); and by grants JA 1830/1-2 and SFB 740, Priority Program 1365, and the German-Israel Project Cooperation DIP (T.S. and E.J.).

Received: July 12, 2013
Revised: October 29, 2013
Accepted: January 24, 2014
Published: March 13, 2014

REFERENCES

Balch, W.E., Morimoto, R.I., Dillin, A., and Kelly, J.W. (2008). Adapting proteostasis for disease intervention. Science *319*, 916–919.

Bernasconi, R., Galli, C., Noack, J., Bianchi, S., de Haan, C.A.M., Reggiori, F., and Molinari, M. (2012). Role of the SEL1L:LC3-I complex as an ERAD tuning receptor in the mammalian ER. Mol. Cell *46*, 809–819.

Bigelow, H., Doitsidou, M., Sarin, S., and Hobert, O. (2009). MAQGene: software to facilitate C. elegans mutant genome sequence analysis. Nat. Methods *6*, 549.

Bordallo, J., Plemper, R.K., Finger, A., and Wolf, D.H. (1998). Der3p/Hrd1p is required for endoplasmic reticulum-associated degradation of misfolded lumenal and integral membrane proteins. Mol. Biol. Cell *9*, 209–222.

Brenner, S. (1974). The genetics of Caenorhabditis elegans. Genetics *77*, 71–94.

Brown, M.K., and Naidoo, N. (2012). The endoplasmic reticulum stress response in aging and age-related diseases. Front. Physiol. *3*, 263.

Cao, S.S., and Kaufman, R.J. (2013). Targeting endoplasmic reticulum stress in metabolic disease. Expert Opin. Ther. Targets *17*, 437–448.

Davis, M.W., Hammarlund, M., Harrach, T., Hullett, P., Olsen, S., and Jorgensen, E.M. (2005). Rapid single nucleotide polymorphism mapping in C. elegans. BMC Genomics *6*, 118.

Douglas, P.M., and Dillin, A. (2010). Protein homeostasis and aging in neurodegeneration. J. Cell Biol. *190*, 719–729.

Eisenberg, T., Knauer, H., Schauer, A., Büttner, S., Ruckenstuhl, C., Carmona-Gutierrez, D., Ring, J., Schroeder, S., Magnes, C., Antonacci, L., et al. (2009). Induction of autophagy by spermidine promotes longevity. Nat. Cell Biol. *11*, 1305–1314.

Fredriksson, Å., Johansson Krogh, E., Hernebring, M., Pettersson, E., Javadi, A., Almstedt, A., and Nyström, T. (2012). Effects of aging and reproduction on protein quality control in soma and gametes of Drosophila melanogaster. Aging Cell *11*, 634–643.

Hamasaki, M., Furuta, N., Matsuda, A., Nezu, A., Yamamoto, A., Fujita, N., Oomori, H., Noda, T., Haraguchi, T., Hiraoka, Y., et al. (2013). Autophagosomes form at ER-mitochondria contact sites. Nature *495*, 389–393.

Hampton, R.Y., Gardner, R.G., and Rine, J. (1996). Role of 26S proteasome and HRD genes in the degradation of 3-hydroxy-3-methylglutaryl-CoA reductase, an integral endoplasmic reticulum membrane protein. Mol. Biol. Cell *7*, 2029–2044.

Henis-Korenblit, S., Zhang, P., Hansen, M., McCormick, M., Lee, S.-J., Cary, M., and Kenyon, C. (2010). Insulin/IGF-1 signaling mutants reprogram ER stress response regulators to promote longevity. Proc. Natl. Acad. Sci. USA *107*, 9730–9735.

Honda, Y., Tanaka, M., and Honda, S. (2010). Trehalose extends longevity in the nematode Caenorhabditis elegans. Aging Cell *9*, 558–569.

Hsu, A.-L., Murphy, C.T., and Kenyon, C. (2003). Regulation of aging and age-related disease by DAF-16 and heat-shock factor. Science *300*, 1142–1145.

Jia, K., and Levine, B. (2010). Autophagy and longevity: lessons from C. elegans. Adv. Exp. Med. Biol. *694*, 47–60.

Johnson, W.G. (2000). Late-onset neurodegenerative diseases—the role of protein insolubility. J. Anat. *196*, 609–616.

Kamath, R.S., and Ahringer, J. (2003). Genome-wide RNAi screening in Caenorhabditis elegans. Methods *30*, 313–321.

Kenyon, C.J. (2010). The genetics of ageing. Nature *464*, 504–512.

Koga, H., Kaushik, S., and Cuervo, A.M. (2011). Protein homeostasis and aging: The importance of exquisite quality control. Ageing Res. Rev. *10*, 205–215.

Kroeger, H., Miranda, E., MacLeod, I., Pérez, J., Crowther, D.C., Marciniak, S.J., and Lomas, D.A. (2009). Endoplasmic reticulum-associated degradation (ERAD) and autophagy cooperate to degrade polymerogenic mutant serpins. J. Biol. Chem. *284*, 22793–22802.

Lapierre, L.R., Gelino, S., Meléndez, A., and Hansen, M. (2011). Autophagy and lipid metabolism coordinately modulate life span in germline-less C. elegans. Curr. Biol. *21*, 1507–1514.

Link, C.D. (1995). Expression of human beta-amyloid peptide in transgenic Caenorhabditis elegans. Proc. Natl. Acad. Sci. USA *92*, 9368–9372.

Link, C.D., Johnson, C.J., Fonte, V., Paupard, M., Hall, D.H., Styren, S., Mathis, C.A., and Klunk, W.E. (2001). Visualization of fibrillar amyloid deposits in living, transgenic Caenorhabditis elegans animals using the sensitive amyloid dye, X-34. Neurobiol. Aging *22*, 217–226.

Meléndez, A., Tallóczy, Z., Seaman, M., Eskelinen, E.L., Hall, D.H., and Levine, B. (2003). Autophagy genes are essential for dauer development and life-span extension in C. elegans. Science *301*, 1387–1391.

Menzies, F.M., Moreau, K., and Rubinsztein, D.C. (2011). Protein misfolding disorders and macroautophagy. Curr. Opin. Cell Biol. *23*, 190–197.

Meusser, B., Hirsch, C., Jarosch, E., and Sommer, T. (2005). ERAD: the long road to destruction. Nat. Cell Biol. *7*, 766–772.

Morley, J.F., and Morimoto, R.I. (2004). Regulation of longevity in Caenorhabditis elegans by heat shock factor and molecular chaperones. Mol. Biol. Cell *15*, 657–664.

Ozcan, L., and Tabas, I. (2012). Role of endoplasmic reticulum stress in metabolic disease and other disorders *63*, 317–328. http://dx.doi.org/10.1146/Annurev-Med-043010-144749.

Parodi, A.J. (2000). Role of N-oligosaccharide endoplasmic reticulum processing reactions in glycoprotein folding and degradation. Biochem. J. *348*, 1–13.

Plemper, R.K., Bordallo, J., Deak, P.M., Taxis, C., Hitt, R., and Wolf, D.H. (1999). Genetic interactions of Hrd3p and Der3p/Hrd1p with Sec61p suggest a retro-translocation complex mediating protein transport for ER degradation. J. Cell Sci. *112*, 4123–4134.

Qin, L., Wang, Z., Tao, L., and Wang, Y. (2010). ER stress negatively regulates AKT/TSC/mTOR pathway to enhance autophagy. Autophagy *6*, 239–247.

Rahman, M.M., Stuchlick, O., El-Karim, E.G., Stuart, R., Kipreos, E.T., and Wells, L. (2010). Intracellular protein glycosylation modulates insulin mediated lifespan in C.elegans. Aging (Albany, N.Y. Online) *2*, 678–690.

Roth, J., Zuber, C., Park, S., Jang, I., Lee, Y., Kysela, K.G., Le Fourn, V., Santimaria, R., Guhl, B., and Cho, J.W. (2010). Protein N-glycosylation, protein folding, and protein quality control. Mol. Cells *30*, 497–506.

Rual, J.F., Ceron, J., Koreth, J., Hao, T., Nicot, A.S., Hirozane-Kishikawa, T., Vandenhaute, J., Orkin, S.H., Hill, D.E., van den Heuvel, S., and Vidal, M. (2004). Toward improving Caenorhabditis elegans phenome mapping with an ORFeome-based RNAi library. Genome Res. *14* (10B), 2162–2168.

Saito, Y., Yamanushi, T., Oka, T., and Nakano, A. (1999). Identification of SEC12, SED4, truncated SEC16, and EKS1/HRD3 as multicopy suppressors of ts mutants of Sar1 GTPase. J. Biochem. *125*, 130–137.

Schipanski, A., Lange, S., Segref, A., Gutschmidt, A., Lomas, D.A., Miranda, E., Schweizer, M., Hoppe, T., and Glatzel, M. (2013). A novel interaction between aging and ER overload in a protein conformational dementia. Genetics *193*, 865–876.

Shen, X., Ellis, R.E., Sakaki, K., and Kaufman, R.J. (2005). Genetic interactions due to constitutive and inducible gene regulation mediated by the unfolded protein response in C. elegans. PLoS Genet. *1*, e37.

Shintani, T., Yamazaki, F., Katoh, T., Umekawa, M., Matahira, Y., Hori, S., Kakizuka, A., Totani, K., Yamamoto, K., and Ashida, H. (2010). Glucosamine induces autophagy via an mTOR-independent pathway. Biochem. Biophys. Res. Commun. *391*, 1775–1779.

Shore, D.E., Carr, C.E., and Ruvkun, G. (2012). Induction of cytoprotective pathways is central to the extension of lifespan conferred by multiple longevity pathways. PLoS Genet. *8*, e1002792.

Taylor, R.C., and Dillin, A. (2013). XBP-1 is a cell-nonautonomous regulator of stress resistance and longevity. Cell *153*, 1435–1447.

Tian, Y., Li, Z., Hu, W., Ren, H., Tian, E., Zhao, Y., Lu, Q., Huang, X., Yang, P., Li, X., et al. (2010). C. elegans screen identifies autophagy genes specific to multicellular organisms. Cell *141*, 1042–1055.

Walter, P., and Ron, D. (2011). The unfolded protein response: from stress pathway to homeostatic regulation. Science *334*, 1081–1086.

Wellen, K.E., Lu, C., Mancuso, A., Lemons, J.M.S., Ryczko, M., Dennis, J.W., Rabinowitz, J.D., Coller, H.A., and Thompson, C.B. (2010). The hexosamine biosynthetic pathway couples growth factor-induced glutamine uptake to glucose metabolism. Genes Dev. *24*, 2784–2799.

Yorimitsu, T., and Klionsky, D.J. (2007). Endoplasmic reticulum stress: a new pathway to induce autophagy. Autophagy *3*, 160–162.

Zhao, Y., Hu, J., Miao, G., Qu, L., Wang, Z., Li, G., Lv, P., Ma, D., and Chen, Y. (2013). Transmembrane protein 208: a novel ER-localized protein that regulates autophagy and ER stress. PLoS ONE *8*, e64228.

Zhou, K.I., Pincus, Z., and Slack, F.J. (2011). Longevity and stress in Caenorhabditis elegans. Aging (Albany NY) *3*, 733–753.